

## Formation of Proteasome–PA700 Complexes Directly Correlates with Activation of Peptidase Activity<sup>†</sup>

George M. Adams,<sup>‡</sup> Brad Crotchett,<sup>‡</sup> Clive A. Slaughter,<sup>§</sup> George N. DeMartino,<sup>||</sup> and Edward P. Gogol<sup>\*,‡</sup>

*School of Biological Sciences, University of Missouri–Kansas City, Kansas City, Missouri 64110, and Howard Hughes Medical Institute and Departments of Biochemistry and Physiology, The University of Texas Southwestern Medical Center, Dallas, Texas 75235*

*Received June 22, 1998*

**ABSTRACT:** The proteolytic activity of the eukaryotic 20S proteasome is stimulated by a multisubunit activator, PA700, which forms both 1:1 and 2:1 complexes with the proteasome. Formation of the complexes is enhanced by an additional protein assembly called modulator, which also stimulates the enzymatic activity of the proteasome only in the presence of PA700. Here we show that the binding of PA700 to the proteasome is cooperative, as is the activation of the proteasome's intrinsic peptidase activity. Modulator increases the extent of complex formation and peptidase activation, while preserving the cooperative kinetics. Furthermore, the increase in activity is not linear with the number of PA700 assemblies bound to the proteasome, but rather with the number of proteasome–PA700 complexes, regardless of the PA700:proteasome stoichiometry. Hence the stimulation of peptidase activity is fully (or almost fully) effected by the binding of a single PA700 to the 20S proteasome. The stimulation of peptidase by modulator is explained entirely by the increased number of proteasome–PA700 complexes formed in its presence, rather than by any substantial direct stimulation of catalysis. These observations are consistent with a model in which PA700, either alone or assisted by modulator, promotes conformational changes in the proteasome that activate the catalytic sites and/or facilitate access of peptide substrates to these sites.

The degradation of most cellular proteins, both to eliminate misfolded or denatured polypeptides and to regulate concentrations of components critical for control of cell cycle and metabolism, is performed by large cytosolic complexes called proteasomes (1, 2). Two assemblies associated with this activity have been isolated and characterized: a core complex of 14 different polypeptides (the 20S proteasome) that exhibits only a relatively low level of activity, limited to peptides and loosely structured proteins (3); and a larger 26S assembly that contains 20 additional regulatory polypeptides (3–5). The 26S proteasome has higher intrinsic proteolytic activity, as well as a wider range of substrates, including ubiquitinated proteins, whose degradation also requires ATP hydrolysis (3). The regulatory proteins themselves form a stable complex, variously called PA700 (6) or 19S (7), that can be isolated, purified, and recombined with the 20S proteasome in a process requiring ATP hydrolysis (6). The reconstituted complex, found in both a 1:1 and a 2:1 ratio of PA700 to 20S proteasome, structurally

resembles the “capped” 26S form of the proteasome, and exhibits both the higher peptidase and protease activities and the ATP-dependent digestion of ubiquitinated substrates characteristic of the 26S complex (8).

Structural analysis of the 20S proteasome has provided important insights into the mechanism of protein digestion. As defined by electron microscopy studies, the 20S proteasome consists of a stack of four heptameric rings of two different families of subunits,  $\alpha$  and  $\beta$ , with the  $\beta$  subunits forming the two internal rings, and the  $\alpha$  subunit rings comprising the ends of the cylindrical structure (9, 10). Crystallographic analysis of both the archeon and eukaryotic 20S proteasome has shown that the catalytic sites, which reside on the  $\beta$  subunits, face a central cavity (11, 12). This elongated cavity is the likely pathway for access of protein substrates to the active sites. Indeed, a protein substrate to which a gold cluster (Nanogold) has been covalently attached has been visualized at the ends of the 20S proteasome, consistent with entry via the central channel (13). However, in the eukaryotic proteasome structure, the ends of the cavity are closed by the N-terminal portions of the  $\alpha$  subunits (12). (The N-termini of the  $\alpha$  subunits are not resolved in the crystal structure of the archaeobacterial 20S.) Hence, substrate access to the active sites by this pathway appears to be obstructed, at least in the state that was isolated and crystallized, and may be a regulatory mechanism for restricting the activity and specificity of the 20S proteasome. Since PA700, as well as an alternative proteasome activator (PA28), binds at the ends of the proteasome (8, 14), it is

<sup>†</sup> This work was supported by grants from the University of Missouri Research Board and the National Institutes of Health (GM57403 to E.P.G. and DK46181 to G.N.D.).

\* Corresponding author: School of Biological Sciences, UM–KC, 5100 Rockhill Rd., Kansas City, MO 64110. (816) 235-2584 (phone); (816) 235-1503 (fax); egogol@cctr.umkc.edu (email).

<sup>‡</sup> School of Biological Sciences, University of Missouri–Kansas City.

<sup>§</sup> Howard Hughes Medical Institute and Department of Biochemistry, the University of Texas Southwestern Medical Center.

<sup>||</sup> Department of Physiology, the University of Texas Southwestern Medical Center.

likely that at least part of its function is to facilitate substrate access into the central channel.

A protein complex of 300 kDa, that has been named modulator, has been identified as a factor that enhances the effects of PA700, at subsaturating PA700 concentrations, but has no observable effect on the proteasome in the absence of PA700 (6). We have shown that the modulator increases the number of PA700 complexes associated with proteasomes, without forming any stable ternary complex detectable by electron microscopy of negatively stained particles (8). The mechanism of promoting this association is not known, nor is it known whether the effect of the modulator is limited to facilitating the assembly of proteasome-PA700 complexes.

Our primary objective in the work reported here is to determine the relationship between formation of proteasome-PA700 complexes and stimulation of catalytic activity, both in the presence and in the absence of the modulator protein complex. Both 1:1 and 2:1 PA700-proteasome complexes are formed at ratios that are dependent on the concentrations of components, including modulator protein, in a process that exhibits a measurable degree of cooperativity (8). The presence of a mixture of states (uncapped and 1:1 and 1:2 complexes) at all concentrations of PA700 has prevented assessment of the functional significance of the stoichiometry of the complexes formed. Here, we correlate a simple measure of proteasome activity (hydrolysis of small peptides) with the distribution of the species of proteasomes, to determine the effects of binding one and two PA700 assemblies. We find that the stimulation of peptidase activity by PA700 exhibits a cooperativity that parallels that seen in the formation of complexes. Correlation of the number and nature of complexes with enzymatic activity indicates that the binding of a single PA700 complex to the proteasome causes maximal, or near-maximal, stimulation of its peptidase activity. We also examine this structure-function relationship in the presence of modulator protein, and find that the same correlation between peptidase activity and capping persists, indicating that the effects of this regulator are explained by its promotion of proteasome-PA700 complex formation.

## MATERIALS AND METHODS

Proteasomes, PA700, and modulator protein were prepared from bovine erythrocytes as previously described (6, 15, 16). Complexes of proteasomes and regulators were formed by incubating 7 nM proteasomes with variable concentrations of PA700 (0–200 nM) in the presence or absence of 15 nM modulator protein in buffer (45 mM Tris-HCl, pH 8.0, 10 mM MgCl<sub>2</sub>, 5 mM dithiothreitol) containing 200  $\mu$ M ATP at 37 °C. Samples were assayed for peptidase activity after incubation times (in the absence of substrate) ranging from 40 to 60 min, yielding no systematic differences among these time points. Electron microscopy specimens were prepared after 40–50 min of incubation of the same samples used for peptidase assay. Several independent preparations of each protein were assayed for activity, all with parallel results, but with the smallest variations in sets of assays all conducted within a 1 day time frame. The total number of specimens used for the correlated activity and structural study was too large to assay and prepare all in 1 day. Hence, to

minimize variability of results, a single preparation of all proteins was used for the data in this work, yielding activity results that were similar to but more internally variable than those obtained in 1 day assays, using the same and different protein preparations.

The chymotrypsin-like peptidase activity of proteasomes was measured by diluting 25  $\mu$ L (or 50  $\mu$ L) of proteasome/PA700 incubation mixture into 500  $\mu$ L (or 1 mL) of buffer (50 mM Tris-HCl, pH 8.0 at 37 °C, 5 mM  $\beta$ -mercaptoethanol) containing 50  $\mu$ M succinyl-Leu-Leu-Val-Tyr-AMC (Bachem Bioscience, Philadelphia, PA) at 37 °C, and following the time course of increase in fluorescence with an SLM Aminco AB2 fluorometer (SLM instruments, Urbana, IL). Activities were measured in triplicate, usually within the first 1–3 min of assay, and hydrolysis was placed on an absolute scale by measuring the end point of digestion of the peptide with chymotrypsin. One unit of activity is defined as a change in concentration of fluorescent product of 1 nM/min.

Electron micrographs were recorded without prior examination of the areas photographed by using minimal dose methods with a JEOL 1200EX microscope. Micrographs were selected for analysis simply on the basis of adequate staining to identify the state (uncapped, 1:1 or 2:1 complexes) of the proteasomes in each field. Micrographs were printed, and particles were visually classified and counted as described (8). For each preparation, approximately 12 micrographs (from 8 to 24) were selected at random and counted, each usually containing 30–60 identifiable proteasomes. At least two different observers counted each preparation to ensure objective agreement.

For statistical analysis of the data, errors were estimated for each type of measurement performed. Errors in enzymatic activity were calculated from the effects of estimated pipetting errors, combined with sample standard deviations obtained from measurements done in triplicate (17). Errors in particle counting were derived from the standard deviations among the dozen individual fields of view analyzed for each data point. Where appropriate, these errors were combined in quadrature. Weighted curve fits were performed using the program Kaleidagraph (Abelbeck Software, Reading, PA).

## RESULTS

**Stimulation of Peptidase Activity.** As reported in the initial isolation and characterization of PA700, addition of PA700 to proteasomes in the presence of ATP results in an increase in proteasome enzymatic activity directed against short synthetic peptides (6). We have repeatedly measured the peptidase activity of the proteasome at various PA700 concentrations, and have detected a sigmoidal behavior with respect to the activator, at constant substrate concentration (Figure 1, open circles). Data from both a single experiment (main figure) as well as the composite of all of the data used for the structure-function correlation (inset) are shown. The data collected in single experiments exhibit smaller deviations from a smooth curve, consistent with its lower estimated errors. However, even the noisier data, representing the specimens used for electron microscopy, show identical behavior with respect to PA700 concentration. In the absence of modulator protein, the activity is half-maximally

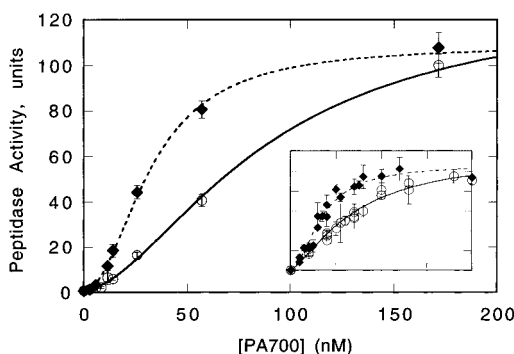


FIGURE 1: Peptidase activity measurements are plotted vs PA700 concentration, and fitted by eq 1. Open circles and the solid curve represent data and their fit in the absence of modulator; filled diamonds and the dashed curve are data and fit in the presence of modulator. Error bars represent one standard deviation, and are estimated from pipetting error estimates and reproducibility of the assay. Main figure: a representative set of data collected in the course of 1 day, using a single dilution of all proteins to minimize errors. Inset: all of the data used for electron microscopy specimens, representing many different protein mixtures prepared at various times. Axes in both figures are identical.

stimulated under the conditions used (7 nM proteasomes, 50  $\mu$ M substrate) at approximately 60 nM PA700.

Addition of modulator protein to the incubation mixture (filled symbols in Figure 1) increases the peptidase activity at subsaturating PA700 concentrations, but without any increase beyond that observed at saturating PA700 (under these conditions, approximately 100 units). The activation of the proteasome is saturated at lower concentrations of PA700 when modulator is present, approximately by a factor of 2–3. The sigmoidal nature of the kinetics of activation persists.

These data have been fitted with the Hill equation (modified by addition of a term for reaction velocity in the absence of activator,  $V_0$ ):

$$V = V_0 + V_{\max}[\text{PA700}]^h / (K + [\text{PA700}]^h) \quad (1)$$

where  $V_{\max}$  is the maximum reaction velocity,  $h$  is the Hill coefficient for activation by PA700 (rather than allosteric substrate interactions), and  $K$  is the apparent binding constant. The fitted curves, with optimized values of the four parameters, are shown in Figure 1 as solid and dashed lines, for the data collected in the absence and presence of modulator. A simpler hyperbolic relationship, corresponding to  $h = 1$  in the above equation, was also fitted to the data (not shown). Evaluation of the  $\chi^2$  statistic for both equations indicates that the sigmoidal fit is valid at the 0.05 significance level or better, whereas a hyperbolic fit is rejected at this or even higher significance level.

The fitted values of  $V_0$  and  $V_{\max}$  correspond to the minimum and maximum values of activity measured, and are similar among all data collected using different protein preparations ( $V_0 = 0.1$ – $0.65$  unit,  $V_{\max} = 98$ – $128$  units). These values did not vary significantly with addition of modulator, consistent with its previously determined lack of effect at zero or saturating concentrations of PA700.

The derived values of the Hill coefficient were in the range of 1.3–2.0, depending on the protein preparation, with standard deviations of 5–10% of the value. The Hill coefficient in general increased with addition of modulator,

though not always significantly. In the single-day experiment shown in Figure 1, for example, modulator causes a change in  $h$  from  $1.7 (\pm 0.1)$  to  $2.0 (\pm 0.1)$ . This observed range of Hill coefficients is consistent with cooperativity between two sites.

The values of  $K$  were not well-determined by curve-fitting, as judged by the large standard deviations of the derived values, up to 70% of their values. The estimated values ranged wildly (from 90 to 2000), and did not exhibit any consistent variation with addition of modulator.

**Cooperativity in Assembly of Complexes.** As seen in our previous examination of the structural effects of PA700 (8), incubation with PA700 transforms a fraction of the proteasomes into singly and doubly “capped” complexes, visible in the electron micrograph in Figure 2. The resulting assemblies have been quantified by classifying all identifiable proteasomes in many fields of view as uncapped (in both end and side views) or as singly or doubly capped. The distribution of these complexes, observed at three subsaturating PA700 concentrations, had previously led us to infer that the association of the caps is cooperative, with an energy of interaction estimated as 0.8 kcal/mol between the two sites (8). Here we have directly tested the cooperativity in assembly by quantifying the fraction of capped proteasome particles over a range of PA700 concentrations (Figure 3). Each data point represents the percentage of capped proteasomes, either singly or doubly capped, in approximately 12 randomly chosen micrographs of a single proteasome—PA700 mixture, either in the absence or in the presence of modulator protein (open and filled symbols, respectively). As we had previously noted, addition of modulator causes an increase in the fraction of capped proteasomes at subsaturating concentrations of PA700.

The scatter of the data in Figure 3 is high, consistent with the relatively large error of each point. These errors were estimated from the variances among the individual micrographs, combined with the estimated errors in protein concentrations. In parallel to the analysis of the peptidase activity measurements, the data in Figure 3 were fitted by the Hill equation:

$$C = C_{\max}[\text{PA700}]^h / (K + [\text{PA700}]^h) \quad (2)$$

where  $C$  is the percentage of proteasomes capped (with either one or two PA700 complexes),  $C_{\max}$  is the maximum percentage, set to 100%,  $h$  is the Hill coefficient for the observed structural change, and  $K$  is the apparent binding constant. The fitted curves (solid and dashed lines) appear to describe the relationship among the data points quite well, considering the high scatter. Calculation of the  $\chi^2$  statistic for the fits of these data to the sigmoidal curves indicates that the fits are superior to the alternative hyperbolic relationship by a factor of 2.3–2.5, indicating that the Hill equation provides the more accurate description of the data. The calculated values of  $\chi^2$  are higher than consistent with normal statistical acceptance levels (e.g., 0.05), suggesting that the errors may be underestimated. Indeed, uniformly raising all error estimates by a factor of 1.5 yields fits for the sinusoidal curves that are significant at the 0.05 level, while the hyperbolic fits are rejected at the 0.001 level. Hence, a sigmoidal relationship is strongly indicated, and



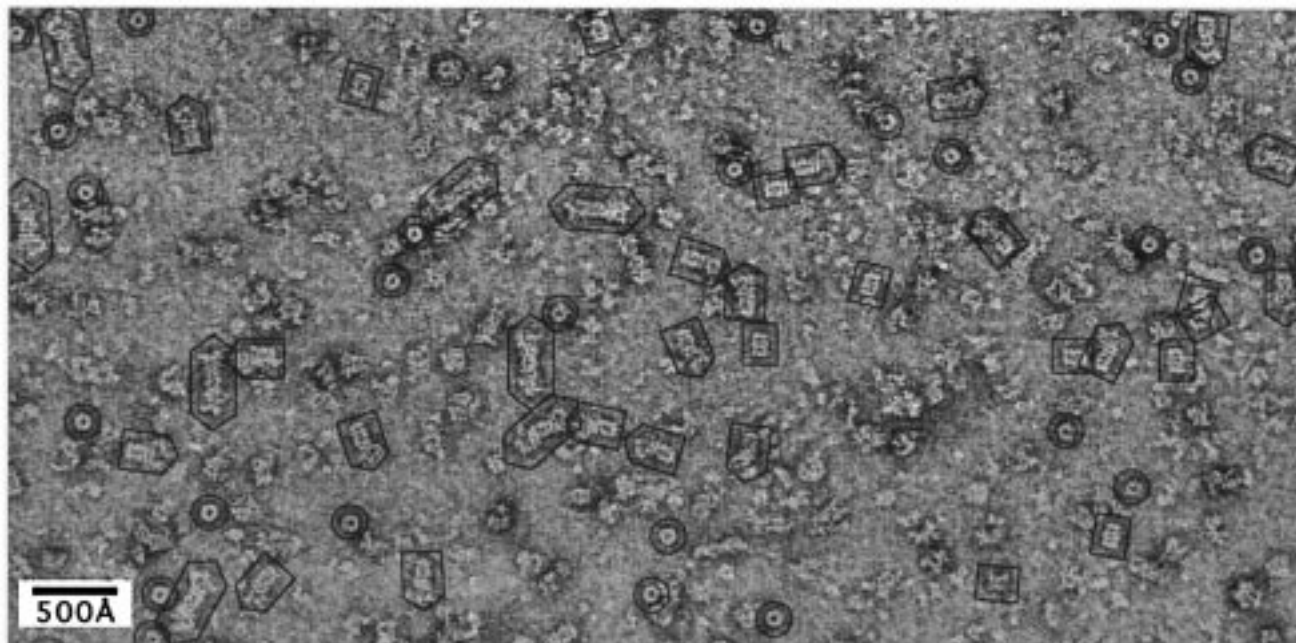


FIGURE 2: Electron micrograph of proteasome-PA700 complexes, with identifiable proteasomes by various outlines: circles, end views; rectangles, side views of uncapped proteasomes; pentagons and hexagons, singly and doubly capped proteasomes, respectively.

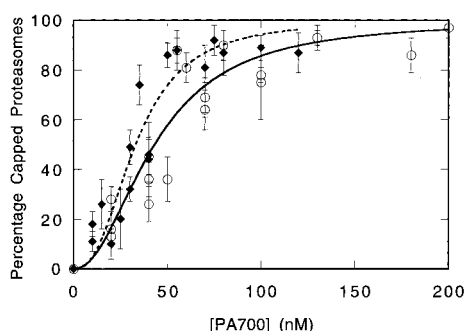


FIGURE 3: Percentages of capped proteasomes are plotted vs PA700 concentration, and fitted by eq 2. Each data point represents all of the particles identified from approximately 12 micrographs of 1 preparation, and error bars indicate 1 standard deviation in the percentages calculated among the individual micrographs. Open circles and the solid curve represent the data and their fit in the absence of modulator; filled diamonds and the dashed curve are the data and fit in the presence of modulator.

cooperativity in the formation of proteasome-PA700 complexes is demonstrated.

The best fit of the Hill equation to the data in Figure 3 yields a value of  $h$  of 2.2 ( $\pm 0.3$  error of fit) for the experiments conducted in the absence of modulator, and 2.4 ( $\pm 0.4$ ) in the presence of modulator. Both of these values for the Hill coefficient are slightly higher than those derived from the corresponding enzymatic activity measurements, but the larger errors in these measurements make the significance of this difference dubious. The other parameter derived from the fits,  $K$ , is not directly comparable between the two experiments, since in the case of activity measurements  $K$  reflects the hydrolysis of substrate, while the  $K$  derived from the electron microscopy measurements relates directly to the affinity between proteasomes and PA700. Due to the higher error level and scatter in the data, the values of  $K$  derived from this analysis are extremely imprecise, having standard deviations larger than their values. Hence, the major conclusion drawn from this analysis is that the

cooperativity determined for activation of the proteasome by PA700, in both the presence and absence of modulator protein, is also present in formation of complexes, and is characterized by similar Hill coefficients.

**Correlation of Activation with Capping.** The central question we aim to address in this work is the relationship between formation of capped complexes and stimulation of enzymatic activity, specifically, the relative contributions of the first and second PA700 complexes that become associated with proteasomes. We have approached this question by examining the correlation between peptidase activity and either fraction of capped proteasome *ends* (half-proteasomes) or fraction of capped *particles*. A model of independent activation of each half-proteasome by binding a PA700 cap, that is, one in which each cap would cause an equivalent level of stimulation of proteolysis, predicts a linear relationship between activity and capped proteasome *ends*. An alternative model of coupled activation, in which the two symmetrical halves of the proteasome act as a unit and are fully activated by addition of a single PA700 cap, is consistent with a linear relationship between activity and fraction of capped *particles*.

These two alternative analyses of the data, both in the absence and in the presence of modulator (open and filled symbols, respectively), are shown in Figure 4A,B, with error bars calculated from standard deviations of both activity and particle counting measurements. (Errors in the abscissa have been converted and combined with the errors in the ordinate.) Both plots show a monotonic increase in activity with each measure of capping. The difference between the two is the *linearity* of each postulated relationship, measured by goodness of fit to the error-weighted least-squares lines drawn for each data set (solid lines without modulator, dashed lines with modulator). Statistical comparisons of the fit of the data to the two alternative linear relationships were done by calculating the  $\chi^2$  statistic for both plots. As listed in Table 1, the linear fits of activity to percentage of capped

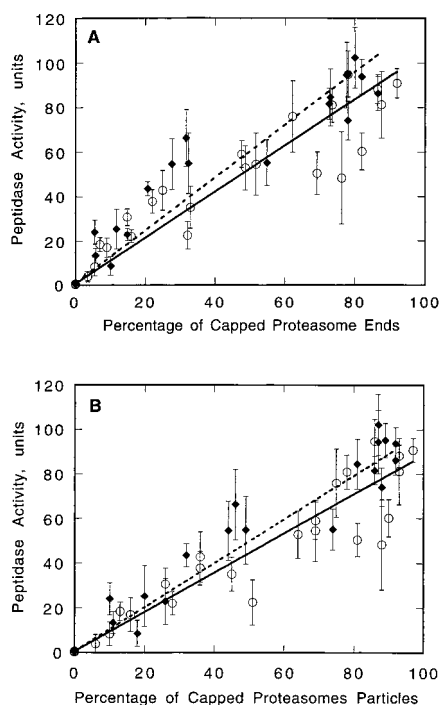


FIGURE 4: Peptidase activity of each preparation is plotted against (A) the percentage of capped proteasomes (either single or double capped) and (B) the percentage of capped proteasome ends (treating each half-proteasome independently). Open circles and solid lines represent data and linear fit in the absence of modulator; filled diamonds and dashed lines are data and fit in the presence of modulator. Error bars represent the root-mean-square summation of errors in both activity and capping (particles or ends). Slopes and goodness-of-fit statistics for all fits are listed in Table 1.

Table 1: Fits of Activity Data to Percentages of Capped Proteasome Ends (Independent End Model: Figure 4A) and Capped Proteasomes (Coupled Model: Figure 4B)

modulator	model			
	independent ends		coupled ends	
	0 nM	15 nM	0 nM	15 nM
slope (error)	1.04 (0.03)	1.20 (0.04)	0.88 (0.03)	0.99 (0.04)
$\chi^2$	69.5	72.1	36.2	24.1
no. of data points	29	19	29	19
$\nu$ (degrees of freedom)	27	17	27	17
$\chi^2/\nu$	2.57	4.24	1.34	1.42
rejection level	<0.001	<0.001	0.2	0.2

proteasome ends (Figure 4A) can be rejected at the 0.001 confidence level, both in the absence and in the presence of modulator. In contrast, the relationship of activity to percentage of capped particles (Figure 4B) is linear in both the absence and presence of modulator at the 0.1 confidence level. Thus, these results indicate that the peptidase activity of proteasome—PA700 complexes is directly dependent on the fraction of capped *particles*, regardless of the number of caps (one or two), rather than the fraction of capped *ends*.

**Effects of Modulator Protein on Activity.** The coordinate effect of the modulator protein on formation of complexes and activation of the proteasome is illustrated by the data and fits of Figure 4B. If the only effect of modulator on the proteasome is to increase its affinity for PA700, complexes formed in the presence of the modulator should have the same activity as in its absence. The observed increase in activity would be due entirely to the increased

fraction of capped proteasomes. The position and scatter of both data sets in Figure 4B are similar, though the slopes of the weighted least-squares fits differ slightly (Table 1). The difference between the slopes ( $0.88 \pm 0.03$  vs  $0.99 \pm 0.04$ ), though outside of estimated errors of fit, is small enough to be questionable. When a single linear fit (not shown) is made to all of the data in Figure 4B, the  $\chi^2$  value calculated is of intermediate significance: it can be rejected at the 0.05 but not at the 0.02 confidence level. Thus, we cannot entirely exclude the possibility of minor secondary effects of the modulator on the proteasome. However, this analysis shows that the major (and possibly only) effect of the modulator in enhancing the PA700-dependent activation is promoting association of PA700 with the proteasome. The small difference between the two data sets in Figure 4B illustrates the magnitude of any possible additional effect.

## DISCUSSION

We have previously shown that the proteasome activator PA700 functionally and structurally modifies the 20S proteasome to give it functional properties and structural appearance indistinguishable from those of the 26S proteasome. It does so by binding at one or both ends in a cooperative manner. In the work presented here, we demonstrate a parallel cooperative activation of enzymatic activity and formation of complexes, as detected by electron microscopy. The measurement of proteasome capping by electron microscopy correlates well with the catalytic behavior of the proteasomes. The parallel dependence of the two processes on PA700 concentration supports the hypothesis that activation of peptidase activity is dependent on formation of proteasome—PA700 complexes. Examination of measures of capping (capped ends vs capped particles) indicates that the peptidase function appears to be fully stimulated by binding of a single PA700 to the proteasome. This effect of one cap on the entire proteasome may reflect the cooperativity exhibited between the two halves of the proteasome for association with PA700.

Though the mechanism of the catalytic activation of the proteasome by PA700 is not known, it may be dissected into two elements: stimulation of the peptidase activity intrinsic to the 20S, and expansion of the range of substrates to include native proteins, both with and without ubiquitylation. Direction toward ubiquitinated proteins is presumably due to the ubiquitin-binding (18) and enzymatic activities of the PA700 subunits, specifically the 37 kDa ubiquitin isopeptidase subunit (19), and the six putative ATPase subunits (20). One role postulated for ATPase activity in the 26S proteasome is unfolding of native protein structure prior to digestion (21), which may be critical for degradation of ubiquitinated proteins. None of these functions has been explored in the simple assay of catalytic activity used in this work, and the results obtained may differ for the more complex process of hydrolysis of protein substrates.

The effect of PA700 on the proteasomes studied in the work reported here is stimulation of the intrinsic catalytic activity of the proteasome, assayed by hydrolysis of peptides. This activation is unlikely to be caused by direct interaction of PA700 regulatory subunits with the proteasome's catalytic  $\beta$  subunits, since PA700 attaches at the ends of the proteasome, and is separated from the  $\beta$  subunits by a ring

of  $\alpha$  subunits. However, it is possible that PA700 binding promotes conformational changes in the catalytic sites of the  $\beta$  subunits that result in stimulation of their catalytic activity. The binding of PA700 to one end of the proteasome may be sufficient to effect such changes in both rings of  $\beta$  subunits. An alternative though not mutually exclusive mechanism for PA700 action is promotion of conformational changes in the outer rings of  $\alpha$  subunits that would facilitate the entry of substrates into the central cavity of the proteasome. These changes may include relief of the obstruction of the cavity by the amino termini of the  $\alpha$  subunits. Again, if both ends of the proteasome are coordinately affected by the binding of a single PA700 complex, the binding of a second PA700 would have no additional effect on peptidase activity. The cooperativity observed in binding of a second PA700 may reflect such a conformational change at the distal end of a singly capped proteasome.

Our previous work demonstrates that the modulator protein enhances the structural transformation of the 20S proteasome by promoting the assembly of complexes with PA700. In the present work, we show that the modulator causes parallel stimulatory effects on both activity and capping. Coordinate analysis of the activity and distribution of capped species is consistent with full stimulation of the proteasome's peptidase activity by binding a single PA700 complex. Furthermore, the majority, and perhaps all, of the enhancement of peptidase activity by modulator is due to promoting formation of proteasome-PA700 complexes, rather than any additional mechanism of catalytic stimulation.

## ACKNOWLEDGMENT

We thank E. E. Wang for assistance with some of the enzymatic assays, and Drs. Joseph Albenesi, Gerald Carlson, and Philip Thomas for critical reading of the manuscript.

## REFERENCES

1. Coux, O., Tanaka, K., and Goldberg, A. L. (1996) *Annu. Rev. Biochem.* 65, 801–847.

2. King, R. W., Deshaies, R. J., Peters, J., and Kirschner, M. W. (1996) *Science* 274, 1652–1658.
3. Waxman, L., Fagan, J. M., and Goldberg, A. L. (1987) *J. Biol. Chem.* 262, 2451–2457.
4. Ugai, S., Tamura, T., Tanahashi, N., Takai, S., Komi, N., Chung, C. H., Tanaka, K., and Ichihara, A. (1993) *J. Biochem.* 113, 754–768.
5. Udvardy, A. (1993) *J. Biol. Chem.* 268, 9055–9062.
6. Ma, C., Vu, J. H., Proske, R. J., Slaughter, C. A., and DeMartino, G. N. (1994) *J. Biol. Chem.* 269, 3539–3547.
7. Peters, J., Franke, W. W., and Kleinschmidt, J. A. (1994) *J. Biol. Chem.* 269, 7709–7718.
8. Adams, G., Falke, S., Slaughter, C. A., DeMartino, G. N., and Gogol, E. P. (1997) *J. Mol. Biol.* 273, 646–657.
9. Pühler, G., Weinkauff, S., Bachmann, L., Müller, S., Engel, A., Hegerl, R., and Baumeister, W. (1992) *EMBO J.* 11, 1607–1616.
10. Peters, J.-M., Cejka, Z., Harris, J. R., Kleinschmidt, J. A., and Baumeister, W. (1993) *J. Mol. Biol.* 229, 932–937.
11. Löwe, J., Stock, D., Jap, B., Zwickl, P., Baumeister, W., and Huber, R. (1995) *Science* 268, 533–539.
12. Groll, M., Ditzel, L., Löwe, J., Stock, D., Bochtler, M., Bartunik, H. D., and Huber, R. (1997) *Nature* 386, 463–471.
13. Wenzel, T., and Baumeister, W. (1995) *Nat. Struct. Biol.* 2, 199–204.
14. Gray, C. W., Slaughter, C. A., and DeMartino, G. N. (1994) *J. Mol. Biol.* 236, 7–15.
15. McGuire, M. J., and DeMartino, G. N. (1989) *Biochem. Biophys. Res. Commun.* 160, 911–916.
16. DeMartino, G. N., Proske, R. J., Moomaw, C. R., Strong, A. A., Song, X., Hisamatsu, H., Tanaka, K., and Slaughter, C. A. (1996) *J. Biol. Chem.* 271, 3112–3118.
17. Bevington, P. R., and Robinson, D. K. (1992) *Data Reduction and Error Analysis for the Physical Sciences*, McGraw-Hill, New York.
18. Deveraux, Q., Ustrell, V., Pickart, C., and Rechsteiner, M. (1994) *J. Biol. Chem.* 269, 7059–7061.
19. Lam, Y. A., Xu, W., DeMartino, G. N., and Cohen, R. E. (1997) *Nature* 385, 737–740.
20. DeMartino, G. N., Moomaw, C. R., Zagnitko, O. P., Proske, R. J., Ma, C.-P., Afendis, S. J., Swaffield, J. C., and Slaughter, C. A. (1994) *J. Biol. Chem.* 269, 20878–20884.
21. Rubin, D., and Finley, D. (1995) *Curr. Biol.* 5, 854–858.

BI981482I